International Journal of Engineering Research & Technology (IJERT)
ISSN: 2278-0181
Vol. 6 Issue 05, May - 2017

Fault Diagnosis of Cracked Beam Structure using Advanced Neuaral Network Techniques

Guru Prasad Khuntia
Accenture Solution Private Ltd
Past: Dept of Mechanical Engineering,
Institute of Technical Education and Research
S'O'A University, Bhubaneswar
Bangalore , India

Dhirendranath Thatoi
Dept. of Mechanical Engineering
Institute Of Technical Education and Research
S'O'A University, Bhubaneswar
Bhubaneswar, Odisha, India

***Abstract*— Recent developments in Artificial Neural Networks (ANNs) have opened up new possibilities in the domain of inverse problems. Inverse problems are extensively used for identification of crack in large structures (such as bridges) , which may lead to premature damage, has been detected at earlier stage. This study has presented a method for estimating the damage intensities of bridge like structures using a back-propagation based artificial intelligence techniques. This paper presents a novel application of genetically programmed artificial features, which are computer crafted, data driven, and possibly without physical interpretation, to the problem of fault detection. Natural frequencies of the beam under the effect of crack have been studied to compare the results with those of a beam without crack. It is observed that the presence of crack results in change of natural frequency and alters beam response patterns. In this paper a design tool ANSYS is used to monitor various changes in vibrational characteristics of thin transverse cracks on a cantilever beam for detecting the crack position and depth and was compared using artificial intelligence techniques. The usage of neural networks is the key point of development in this paper. The three neural networks used are cascade forward back propagation (CFBP) network, feed forward back propagation (FFBP) network, and radial basis function (RBF) network. In the first phase of this paper theoretical analysis has been made and then the finite element analysis has been carried out using commercial software, ANSYS. In the second phase of this paper the neural networks are trained using the values obtained from a simulated model of the actual cantilever beam using ANSYS. At the last phase a comparative study has been made between the data obtained from neural network technique and finite element analysis.**

Keywords*— Vibration, Mode Shapes, Stress intensity factor, ANSYS.

1. INTRODUCTION

Crack is one of the most common defects in structures that may result in adverse effects on the behavior and ill performance of structures, which can eventually lead to their collapse. Cracks induce changes in the structure's stiffness, also reducing its natural frequency. Crack has the tendency to open and close in time depending on the load on beam. The main factor for causing crack is the static deflection on the structures body weight, which may cause the beam to open at all the time or partially leading to premature damage to the beam. The major factor that affects the crack is vibrational amplitude. If the static deflection is larger than the vibrational amplitude then the crack remains open, and vice versa. Various studies over the last decade have indicated that a beam with a breathing crack, i.e., one which opens and closes during oscillation, shows nonlinear dynamic behavior because of the variation in the structural stiffness which occurs during the response cycle. On the other hand, the effect of moving loads and masses on structures and machines is an important problem both in the field of transportation and in the design of machining processes. A moving load (or moving mass) produces larger deflections and higher stresses than does an equivalent load applied statically. These deflections and stresses are functions of both time and speed of the moving loads. It is, therefore, essential to detect and control damages in structures subjected to a moving mass. Very few studies have been reported in the literatures that deal with moving load or moving mass problems under the effect of cracks. The purpose of the present work is to establish a method for predicting the location and depth of a crack in a cantilever beam using vibration data.

Diagnosing a cracked component by examining the vibration signals is the most commonly used method for detecting this fault. The fault detection is possible by comparing the signals of a machine running in normal and faulty conditions. Depending on the crack's size and location, the stiffness of the structure is reduced and, therefore, so are its natural frequencies compared to the original crack-free structure. This shift in natural frequencies has been commonly used to investigate the crack's location and size.

Vibration analysis can also be carried out using Fourier transform techniques like Fourier series expansion (FSE), Fourier integral transform (FIT) and discrete Fourier transform (DFT). Identification and diagnosis of crack in inaccessible machine member has gained importance in now a day using vibrational analysis and artificial intelligence technologies. Using modern technology sensor is placed near inaccessible internal machine component. The piezoelectric transducer of sensor produces vibrational signal which is transformed using Wavelet Transformation technology. These signals are time & frequency dependent. After extracting fault features, a proper artificial neural network is implemented for

International Journal of Engineering Research & Technology (IJERT)
ISSN: 2278-0181
Vol. 6 Issue 05, May - 2017

aiding of the fault classification. An intelligent fault diagnosis system is performed throughout combing the approach to fault diagnosis with an artificial neural network. An artificial neural network is proved as a reliable technique to diagnose the condition of a rotating member. In general, the cracks present in beams are not always open or close condition. It always varies time to time depending upon the situation. If the loads are static like load due to dead weight, load of the beam etc. and if the deflection is more than the vibration amplitude then the crack becomes a open crack, otherwise it will be breathing crack.

Beams are one of the most commonly used structural elements in several engineering applications and experience a wide variety of static and dynamic loads. Cracks may develop in beam-like structures due to such loads. Considering the crack as a significant form of such damage, its modeling is an important step in studying the behavior of damaged structures. Knowing the effect of crack on stiffness, the beam or shaft can be modeled using either Euler-Bernoulli or Timoshenko beam theories. The beam boundary conditions are used along with the crack compatibility relations to derive the characteristic equation relating the natural frequency, the crack depth and location with the other beam properties.

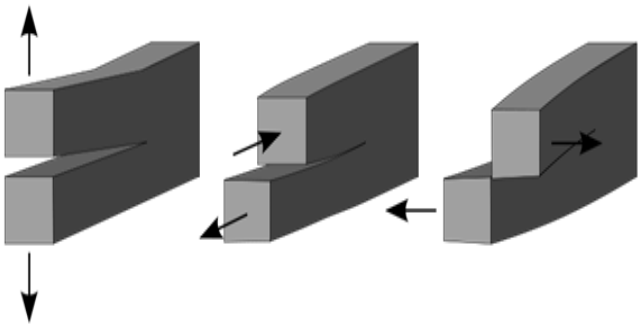

Mode I:Opening Mode II :In-Shear plane Mode III: Out of Shear plane

Fig 1. Different Mode of Crack propagation

Thatoi.et.al [1] suggested that, Condition monitoring and fault detection through vibration analysis applying a pool of analytical and experimental techniques is of continuous attention of researchers. The effectiveness and applicability of each technique has both advantages and limitations. There are various methods being employed for the detection of cracks such as Finite Element Method (FEM), Wavelet analysis, Experimental and Numerical methods, Artificial Intelligence (AI) techniques, other optimization algorithm methods such as Particle Swarm Optimization (PSO) algorithm, Ant Colony Optimization technique (ACO) and Bee Colony Optimization (BCO) algorithm. AI technique will continue to remain one of the favorite analytical tools to extract features automatically in fault diagnosis due to its precise, reliable and low cost solution nature. Cao et al. [2] suggested that, the principle of the model was demonstrated using an Euler–Bernoulli beam component (EBC). As proof-of-concept validation, a fine crack in an EBC was identified with satisfactory precision using the model, in both numerical simulation and experiment. Pawar et al.[3] have performed a composite matrix cracking model, which is implemented in a thin-walled hollow circular cantilever beam using an effective stiffness approach. Using these changes in frequencies due to matrix cracking.

Taghi et al.[4] have proposed a method in which damage in a cracked structure was analyzed using genetic algorithm technique. For modeling the cracked-beam structure an analytical model of a cracked cantilever beam was utilized and natural frequencies were obtained through numerical methods. A genetic algorithm is utilized to monitor the possible changes in the natural frequencies of the structure. The identification of the crack location and depth in the cantilever beam was formulated as an optimization problem. Maity and Saha [5] have presented a method called damage assessment in structures from changes in static parameter using neural network. The basic strategy applied in this study was to train a neural network to recognize the behavior of the undamaged structure as well as of the structure with various possible damaged states. When this trained network was subjected to the measured response; it was able to detect any existing damage. The idea was applied on a simple cantilever beam. Strain and displacement were used as possible candidates for damage identification by a back propagation neural network and the superiority of strain over displacement for identification of damage has been observed. Structural damage detection using neural network with learning rate improvement performed by Fang et al.[6] In this study, he has been explore the structural damage detection using frequency response functions (FRFs) as input data to the back-propagation neural network (BPNN).Neural network based damage detection generally consists of a training phase and a recognition phase. Perera et al. [7] used genetic algorithm for solving multi objective optimization to detect damage. They compared GA optimization based on aggregating functions with pare to optimality. Sahoo and Maity [8] stated that artificial neural networks (ANN) have been proved to be an effective alternative for solving the inverse problems because of the pattern-matching capability. But there is no specific recommendation on suitable design of network for different structures and generally the parameters are selected by trial and error, which restricts the approach context dependent. A hybrid neuro-genetic algorithm is proposed in order to automate the design of neural network for different type of structures. The neural network is trained considering the frequency and strain as input parameter and the location and amount of damage as output parameter. Damage detection methods of structures based on changes in their vibration properties have been widely employed during the last two decades. Existing methods include those based on examination of changes in natural frequencies, mode shapes or mode shape curvatures. An identification procedure to determine the crack characteristics (location and size of the crack) from dynamic measurements has been developed and tested by Shen and Taylor [9]. This procedure is based on minimization of either the “mean-square” or the “max” measure of difference between measurement data (natural frequencies and mode shapes) and the corresponding predictions obtained from the computational model. Necessary conditions are obtained for both formulations. The method is tested for simulated damage in the form of one-side or symmetric cracks in a simply supported Bernoulli-Euler beam.

International Journal of Engineering Research & Technology (IJERT)
ISSN: 2278-0181
Vol. 6 Issue 05, May - 2017

The sensitivity of the solution of damage identification to the values of parameters that characterize damage is discussed. Two approaches are herein presented: The solution of the inverse problem with a power series technique (PST) and the use of artificial neural networks (ANNs). Cracks in a cantilever Bernoulli Euler (BE) beam and a rotating beam are detected by means of an algorithm that solves the governing vibration problem of the beam with the PST. The ANNs technique does not need a previous model, but a training set of data is required. It is applied to the crack detection in the cantilever beam with a transverse crack. The first methodology is very simple and straightforward, though no optimization is included. It yields relative small errors in both the location and depth detection. When using one network for the detection of the two parameters, the ANNs behave adequately and not as an independent document. Please do not revise any of the current designations.

2. MATHEMATICAL FORMULATION

Computation of flexibility matrix of a damaged beam subjected to complex loading. A beam with cracks has smaller stiffness than a normal beam. This decreased local stiffness can be formulated as a matrix. The dimension of the matrix would depend on the degrees of freedom in the problem. Figure 1 shows a cantilever beam of width W and height T, having a transverse surface crack of depth b1. The beam experiences combined longitudinal and transverse motion due to the axial force P1 and bending moment P2. Here we consider two degrees of freedom, leading to a 2*2 local stiffness matrix.

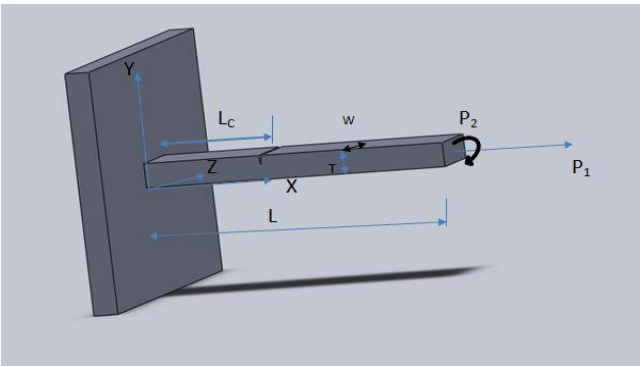

Fig. 2: Beam Model

The relationship between strain energy release rate J (b) and stress intensity factors (G_{Ij}) at the crack section is given by Tada et al. (69) as;

$$J(b) = \frac{1}{E'}(G_{I1} + G_{I2})^2 \qquad (1)$$

Where, $E' = \frac{E}{(1-\nu^2)}$, for plane strain condition and $E' = E$, for plane stress (2)

G_{11} = Stress intensity factor for opening mode I due to load P_1

G_{12} = Stress intensity factor for opening mode I due to load P_2

From earlier studies (Tada et al.,[69]), the values of stress intensity factors are;

$$G_{I1} = \frac{P_1}{WT}\sqrt{\pi b}\left(F_1\left(\frac{b}{T}\right)\right) \quad , \quad G_{I2} = \frac{6P_2}{WT}\sqrt{\pi b}(F_2(\frac{b}{T})) \qquad (3)$$

Where, $0 \le b \le b_1$

Where the experimentally determined functions F1 and F2 are expressed as follows

$$F_1\left(\frac{b}{T}\right) = \left\{\frac{2T}{\pi b}\tan\left(\frac{\pi b}{2T}\right)\right\}^{0.5}\left(\frac{0.752 + 2.02\left(\frac{b}{T}\right) + 0.37(1-\sin\left(\frac{\pi b}{2T}\right))^3}{\cos\left(\frac{\pi b}{2T}\right)}\right)$$

$$F_2\left(\frac{b}{T}\right) = \left\{\frac{2T}{\pi b}\tan\left(\frac{\pi b}{2T}\right)\right\}^{0.5}\left(\frac{0.923 + 0.199(1-\sin\left(\frac{\pi b}{2T}\right))^4}{\cos\left(\frac{\pi b}{2T}\right)}\right)$$

The strain energy release rate (also called strain energy density function) at the crack location is defined as

$J(b) = \frac{\partial U_t}{\partial(b \times W)}$, Where (b × W) is the newly created surface area of the crack. (4)

$$\Rightarrow dU_t = J(b)d(b \times W) = WJ(b)db, \qquad (5)$$

Since the width of the cross section of the beam is constant.

$$U_t = W\int_0^{b_1} J(b)db \qquad (6)$$

So the strain energy release (Ut) due to the crack of depth b1 is calculated as, then from Castigliano's theorem, the additional displacement along the force P_i is:

$$S_i = \frac{\partial U_t}{\partial P_i} \qquad (7)$$

From (1) and (2), thus we have

$$S_i = \frac{\partial}{\partial P_i}[W\int_0^{b_1} J(b)db\,] = W\frac{\partial}{\partial P_i}\left[\int_0^{b_1} J(b)db\right] \qquad (8)$$

$$C_{ij} = \frac{\partial S_i}{\partial P_j} = \frac{\partial}{\partial P_j}[W\frac{\partial}{\partial P_i}\left\{\int_0^{b_1} J(b)db\right\}] = W\frac{\partial^2}{\partial P_i\,\partial P_j}\int_0^{b_1} J(b)db \qquad (9)$$

The flexibility influence co-efficient Cij will be, by definition Substituting equation (1) in equation (5), we have

$$C_{ij} = \frac{W}{E'}\frac{\partial^2}{\partial P_i\,\partial P_j}\int_0^{b_1}(G_{I1} + G_{I2})^2 db \qquad (10)$$

Putting $\delta = \left(\frac{b}{T}\right)$, $d\delta = \left(\frac{db}{T}\right)$,

We get db = Tdδ and when b = 0, δ = 0, b=b_1 $\delta = \left(\frac{b_1}{T}\right) = \delta_1$

From the above condition equation (6) converts to,

International Journal of Engineering Research & Technology (IJERT)
ISSN: 2278-0181
Vol. 6 Issue 05, May - 2017

$$C_{ij} = \frac{WT}{E'}\frac{\partial^2}{\partial P_i \partial P_j}\int_0^{\delta_1}(G_{I1} + G_{I2})^2 d\delta \quad (11)$$

Equation (7) will give different expressions of flexibility influence coefficient Cij.

Cij = flexibility influence coefficient in i direction (x-direction or y-direction) due to the load in j direction (P1 or P2)

Calculating $C_{11} = C_{12}(= C_{21})$ *and* C_{22} *we get*,

$$C_{11} = \frac{WT}{E'}\int_0^{\delta_1}\frac{\pi b}{W^2T^2}2F_1^2(\delta)d\delta = \frac{2\pi}{E'}\int_0^{\delta_1}\delta F_1^2(\delta)d\delta \quad (12)$$

$$C_{12} = C_{21} = \frac{12\pi}{E'TW}\int_0^{\delta_1}\delta F_1(\delta)\,F_2(\delta)d\delta \quad (13)$$

$$C_{22} = \frac{72\pi}{E'WT^2}\int_0^{\delta_1}\delta F_2^2(\delta)d\delta \quad (14)$$

The local stiffness matrix can be obtained by taking the inversion of compliance matrix i.e. ,

$$K = \begin{bmatrix} K_{11} & K_{12} \\ K_{21} & K_{22} \end{bmatrix} = \begin{bmatrix} C_{11} & C_{12} \\ C_{21} & C_{22} \end{bmatrix}^{-1}$$

Converting the influence co-efficient into dimensionless form we get

$$\overline{C_{11}} = C_{11}\frac{WE'}{2\pi};\ \overline{C_{12}} = C_{12}\frac{WE'T}{12\pi} = \overline{C_{21}};\ \overline{C_{22}} = C_{22}\frac{WE'T^2}{72\pi}$$

Governing equations for vibration mode of the cracked beam

The cantilever beam as mentioned in section 2.1 is being considered for free vibration analysis. A cantilever beam of length 'L' width 'W' and depth 'T', with a crack of depth 'b1' at a distance 'Lc' from the fixed end is considered as shown in Figure 1. Taking S1(x, t) and S2(x, t) as the amplitudes of longitudinal vibration for the sections before and after the crack position and V1(x, t), V2(x, t) are the amplitudes of bending vibration for the same sections as shown in Figure 2.

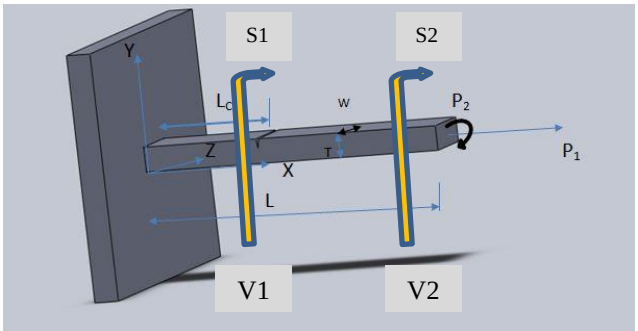

Fig. 3: Beam model with deflection

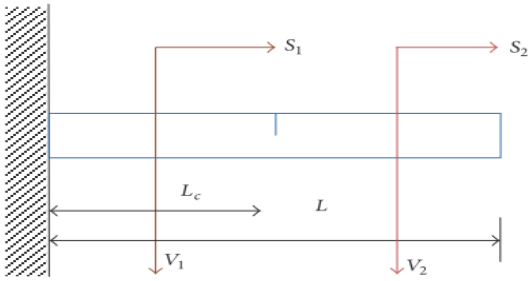

Fig. 4 : Front view of beam model with deflection

The free vibration of an Euler-Bernoulli beam of a constant rectangular cross section is given by the following differential equations as:

$$\frac{\partial^2 S}{\partial t^2} = \left(\frac{E}{\rho}\right)\frac{\partial^2 S}{\partial x^2} \quad \text{for longitudinal vibration and}$$

$$EI\frac{\partial^4 V}{\partial x^4} - \rho\omega^2 V = 0 \quad \text{for lateral vibration of beam}$$

The normal functions for the cracked beam in non-dimensional form for both the longitudinal and bending vibration in steady state can be defined as;

$$\overline{S_1}(\bar{x}) = B_1\cos(\overline{H_S}\bar{x}) + B_2\sin(\overline{H_S}\bar{x}) \quad (15)$$

$$\overline{S_2}(\bar{x}) = B_3\cos(\overline{H_S}\bar{x}) + B_4\sin(\overline{H_S}\bar{x}) \quad (16)$$

$$\overline{V_1}(\bar{x}) = B_5\cosh(\overline{H_v}\bar{x}) + B_6\sinh(\overline{H_v}\bar{x}) + B_7\cosh(\overline{H_v}\bar{x}) + B_8\sinh(\overline{H_v}\bar{x}) \quad (17)$$

$$\overline{V_2}(\bar{x}) = B_9\cosh(\overline{H_v}\bar{x}) + B_{10}\sinh(\overline{H_v}\bar{x}) + B_{11}\cosh(\overline{H_v}\bar{x}) + B_{12}\sinh(\overline{H_v}\bar{x}) \quad (18)$$

Where $\bar{X} = \frac{X}{L}, \bar{S} = \frac{S}{L}, \bar{V} = \frac{V}{L}, \alpha = \frac{L_C}{L}$

$$\overline{H_S} = \frac{\omega L}{D},\quad \overline{D_S} = \left(\frac{E}{\rho}\right)^{1/2},\quad \overline{H_V} = \left(\frac{\omega L^2}{D_V}\right)^{\frac{1}{2}},\quad \overline{D_V} = \left(\frac{EI}{\mu}\right)^{1/2},\quad \mu = A\rho$$

B_i (i=1,2)constants are to be determined ,from boundary conditions.

The boundary condition of cantilever beam in consideration is

$$\overline{S_1}(0) = 0; \overline{V_1}(0) = 0; \overline{V_1}'(0) = 0; \overline{S_2}'(1) = 0; \overline{V_2}''(1) = 0; \overline{V_2}'''(1) = 0$$

At the cracked section:

$$\overline{S_1}(\alpha) = \overline{S_2}(\alpha); \overline{V_1}(\alpha) = \overline{V_2}(\alpha); \overline{V_1}''(\alpha) = \overline{V_2}''(\alpha); \overline{V_1}'''(\alpha) = \overline{V_2}'''(\alpha);$$

Also a S2 acked section, we have:

$$AE\frac{dS_1(L_C)}{dx} = K_{11}(S_2(L_C) - S_2(L_C)) + K_{12}\left(\frac{dV_2(L_C)}{dX} - \frac{dV_1(L_C)}{dX}\right)$$

Multiplying both sides of the above equation by $\frac{AE}{LK_{11}K_{12}}$ we get;

$$N_1N_2\overline{S_1}'(\alpha) = N_2(\overline{S_2}(\alpha) - \overline{S_1}(\alpha)) + N_1(\overline{V_2}'(\alpha) - \overline{V_1}'(\alpha))$$

Similarly,

V2

International Journal of Engineering Research & Technology (IJERT)
ISSN: 2278-0181
Vol. 6 Issue 05, May - 2017

$$EI\frac{d^2V_1(L_C)}{dx^2} = K_{21}(S_2(L_C) - S_1(L_C)) + K_{22}(\frac{dV_2(L_C)}{dx} - \frac{dV_1(L_C)}{dx}) \quad (19)$$

Multiplying both sides of the above equation by $\frac{EI}{L^2K_{11}K_{12}}$,we get,

$$N_3N_4\bar{V_1}''(\alpha) = N_3(\bar{S_2}(\alpha) - \bar{S_1}(\alpha)) + N_4(\bar{V_2}'(\alpha) - \bar{V_1}'(\alpha))$$

Where,

$$N_1 = \frac{AE}{LK_{11}}, N_2 = \frac{AE}{K_{12}}, N_3 = \frac{EI}{LK_{22}}, N_4 = \frac{EI}{L^2K_{21}}$$

The normal functions, equation (11) along with the boundary conditions as mentioned above, yield the characteristic equation of the system as:

$|Q| = 0$

Where Q is a 12 ×12 matrix whose determinant is a function of natural circular frequency (ω), the relative location of the crack (α) and the local stiffness matrix (K) which in turn is a function of the relative crack depth $\delta_1 = \left(\frac{b_1}{T}\right)$. Matrix is given below:

$$Q = \begin{bmatrix} 0 & 0 & 1 & 0 & 0 & 0 & 0 & 0 & 0 & 0 & 0 & 0 \\ 0 & 1 & 0 & 1 & 0 & 0 & 0 & 0 & 0 & 0 & 0 & 0 \\ 0 & 0 & 0 & 0 & G_3 & G_4 & -G_7 & -G_8 & 0 & 0 & 0 & 0 \\ 0 & 0 & 0 & 0 & G_4 & G_3 & G_8 & -G_7 & 0 & 0 & 0 & 0 \\ G_1 & G_2 & -G_5 & -G_6 & -G_1 & -G_2 & G_5 & G_6 & 0 & 0 & 0 & 0 \\ G_2 & G_1 & G_6 & -G_5 & -G_2 & -G_1 & -G_6 & G_5 & 0 & 0 & 0 & 0 \\ G_1 & G_2 & G_5 & G_6 & -G_1 & -G_2 & -G_5 & -G_6 & 0 & 0 & 0 & 0 \\ S_1 & S_2 & S_3 & S_4 & -G_2 & -G_1 & G_6 & -G_5 & S_5 & S_6 & S_7 & S_8 \\ 0 & 0 & 0 & 0 & 0 & 0 & 0 & 0 & 1 & 0 & 0 & 0 \\ 0 & 0 & 0 & 0 & 0 & 0 & 0 & 0 & 0 & 0 & -T_8 & T_7 \\ 0 & 0 & 0 & 0 & 0 & 0 & 0 & -T_6 & & T_5 & T_6 & -T_5 \\ S_9 & S_{10} & S_{11} & S_{12} & S_{13} & S_{14} & S_{15} & S_{16} & S_{17} & S_{18} & -T_5 & -T_6 \end{bmatrix}$$

Where,

$$S_1 = G_2 + N_3\overline{H_V}G_1,\ S_2 = G_1 + N_3\overline{H_V}G_2,$$

$$S_3 = -G_6 - N_3\overline{H_V}G_5,\ S_4 = G_5 - N_3\overline{H_V}G_6,$$

$$S_5 = \frac{N_{34}}{\overline{H_V}}T_5\ \ S_6 = \frac{N_{34}}{\overline{H_V}}T_6,\ S_7 = \frac{-N_{34}}{\overline{H_V}}T_5,$$

$$S_8 = \frac{-N_{34}}{\overline{H_V}}T_6,\ S_9 = N_{12}H_VG_2,\ S_{13} = -N_{12}H_VG_2$$

$$S_{10} = N_{12}\overline{H_V}G_1,\ S_{11} = -N_{12}\overline{H_V}G_6,\ S_{12} = N_{12}\overline{H_V}G_5$$

$$S_{14} = -N_{12}\overline{H_V}G_1,\ S_{15} = N_{12}\overline{H_V}G_6,\ S_{16} = -N_{12}\overline{H_V}G_5$$

$$S_{17} = T_5 - N_1\overline{H_S}T_6,\ S_{18} = T_6 - N_1\overline{H_S}T_5,$$

$$G_1 = \cosh(\overline{H_V}\alpha),\quad G_2 = \sinh(\overline{H_V}\alpha),$$

$$G_3 = \cosh(\overline{H_V}),$$

$$G_4 = \sinh(\overline{H_V}),\ G_5 = \cos(\overline{H_V}\alpha),\quad G_6 = \sin(\overline{H_V}\alpha),$$

$$G_7 = \cosh(\overline{H_V}),\ G_8 = \sin(\overline{H_V}),\ T_5 = \cos(\overline{H_S}\alpha)$$

$$T_6 = \sin(\overline{H_S}\alpha),\ T_7 = \cos(\overline{H_S})$$

$$T_8 = \sin(\overline{H_S}),\quad N_{12} = \frac{N_1}{N_2},\quad N_{34} = \frac{N_3}{N_4}$$

3 . PROCESS OF DETECTING CRACK BY ARTIFICIAL NEURAL NETWORK

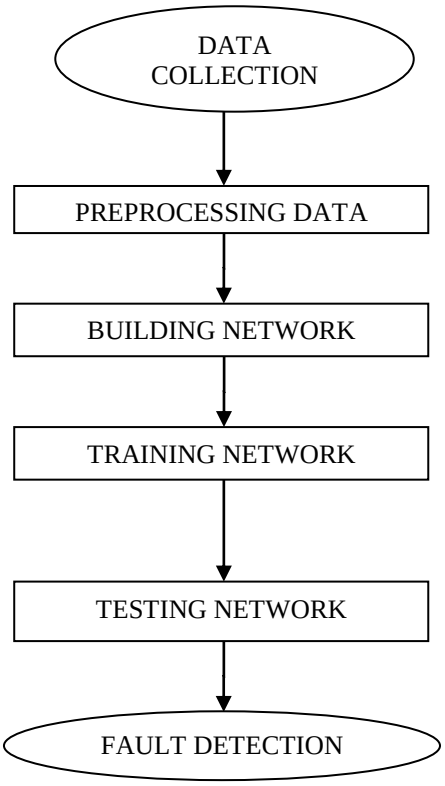

Fig.5: Basic flow diagram of Artificial Neural Network

4. CRACKED BEAM ANALYSIS USING ANSYS

The vibrational analysis of a continuous beam by analytical procedures is quite appropriate and less complicated. How- ever, with the introduction of crack in a beam the analysis of the beam for its vibrational characteristics becomes more complicated. Since the equation of motion of the continuous beam is a partial differential equation and we have with us various initial and boundary conditions we use the finite element method (FEM), which translates the complex partial differential equations into linear algebraic equations and hence the mode of solution becomes simpler.

In the present research the ANSYS is used as a tool to model and simulate a beam with a crack, to monitor the variation in its vibrational characteristics. ANSYS offers engineering simulation solution sets in engineering simulation that a design process requires. Companies in a wide variety of industries use ANSYS software. The tools put a virtual product through a rigorous testing procedure (such as crashing a car into a brick wall, or running for several years on a tarmac road) before it becomes a physical object.

International Journal of Engineering Research & Technology (IJERT)
ISSN: 2278-0181
Vol. 6 Issue 05, May - 2017

The beam is modeled using design software such as solid work and it is imported to ANSYS for the analysis of dimension 800x50x8mmof material generated steel. A crack was inserted in the beam at different locations and of different depths as mentioned below. That cracked beam was subjected to vibration and the frequency for mode-1, mode-2, and mode-3 were noted. Graphs for mode-1, mode-2, and mode-3 were plotted as given below.

5. INTRODUCTION TO NEURAL NETWORK

In order to determine the crack parameters from the frequency data we take the help of artificial intelligence in the form of neural network. The structure of a neural net is very similar to the exact biological structure of a human brain cell. In order to be precise, neural network can be stated as a network model whose functionality is similar to that of the brain. In other words, a neural network is at first trained to recognize a predefined pattern or an already known relationship from certain pre found values. It works by taking certain number of inputs and computing the output after carefully adjusting the weights, which are attached with the input values to differentiate these input values on the basis of importance and priority in processing. These weight values are utilized to obtain the final output. For example, if we have two inputs X_1 and X_2 ,then a simple neural network can be designed and the net input can be found out as

$$Y_{in} = X_1 w_1 + X_2 w_2, \quad (20)$$

where X_1 and X_2 are the activations of the input neurons X_1 and X_2, that is, the output of the input signals. The output of the output neuron can be obtained by applying activations over the net input, that is, the function of the net input:

Y = (Y_{in}), Output = Function (net input calculated).

The function to be applied over the net input is called an activation function. A neural network is classified on the basis of the model's synaptic interconnections, the learning rule adapted and the activation functions used in the neural net. Based on the synaptic interconnections we choose a multilayer perceptron model for our research purpose. Now, depending on the process of learning a neural network, it is classified as supervised learning network, unsupervised learning network, and reinforced learning network. Supervised learning process requires a set of already known values to train the network and hence find out the output. From the set of values obtained after monitoring the vibrational characteristics of the cracked beam and subjecting it to finite element modeling, the corresponding values are trained to the network. The tan sigmoid hyperbolic function is chosen as the activation function. Finally the cascade forward back propagation (CFBP) network model, the feed forward back propagation (FFBP) network model, and the radial basic function (RBF) network model are used and the results are analyzed.

5.1. The CFBP Network.

As stated earlier in the present study a CFBP network is used. This network is very similar to the feed forward back propagation networks with the difference being that the input values calculated after every hidden layer are back-propagated to the input layer and the weights adjusted subsequently. The input values are directly connected to the final output and a comparison occurs between the values obtained from the hidden layers and the values obtained from the input layers and weights are adjusted accordingly. Sahoo et al. [10] and Gopi krishnan et al. [11] observed that the results obtained from CFBP networks are much more efficient than the FFBP networks. Badde et al. [12] suggested that CFBP networks show better and efficient results in most cases.

The algorithm followed in the present paper is given as follows.

(1) Initialize the predefined input matrix.

(2) Initialize the desired output or target matrix.

(3) Initialize the network by using the net = newcf (Input, Output, Hidden layers, Transfer Function, Training algorithm, Learning Function, Performance Function).

(4) Define the various training parameters such as number of epochs, number of validation checks, and maximum and minimum gradient.

(5) Test the new found weights and biases for accuracy.

(6) Using the weights and biases determine the unknown results.

The initial weight and bias values are taken as 0 (zero).

In Figure 1, the inputs are connected to the hidden layer as well as the output layer.

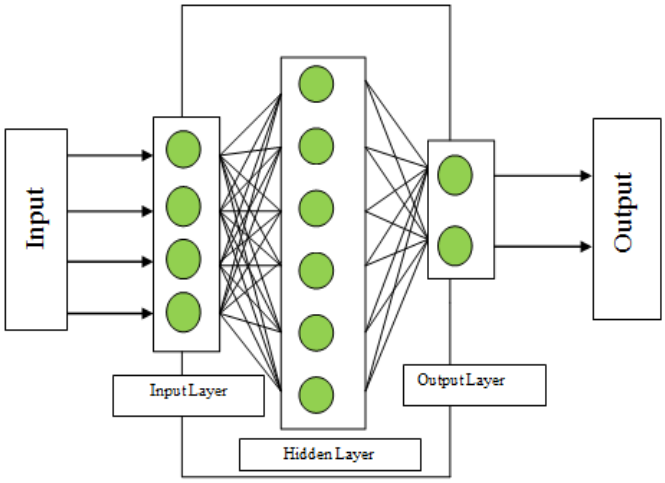

Fig. 6: Structure of CFBP Network

5.2 The FFBP Network.

Another network that we are using for our comparative study in the detection of cracks in a cantilever beam is the feed forward back propagation (FFBP) network (Figure 6). This network differs from the CFBP network on the basis that each subsequent layer has a weight coming from the previous layer and no connection is made between the layers and the first layer. All layers have biases. The last layer is the network output. In this study relevant information comparing the results of both networks as well as the result from a third network is presented. The algorithm used for CFBP network is also used in case of the FFBP network except for the network creation mode, which uses the keyword newff.

International Journal of Engineering Research & Technology (IJERT)
ISSN: 2278-0181
Vol. 6 Issue 05, May - 2017

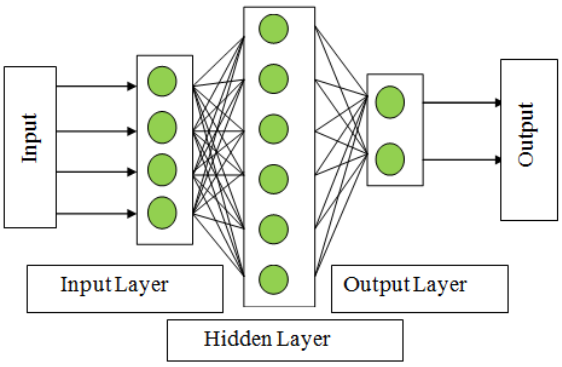

Fig 7: Structure of FFBP Network

5.3 The RBF Network

The radial basis function (RBF) network (Figure 7) is basically used to find the least number of hidden layers or neurons in a single hidden layer, until a minimum error value is reached. The RBF networks can be used to approximate functions. For network creation the keyword newrb adds neurons to the hidden layer of a radial basis network until it meets the specified mean squared error goal.

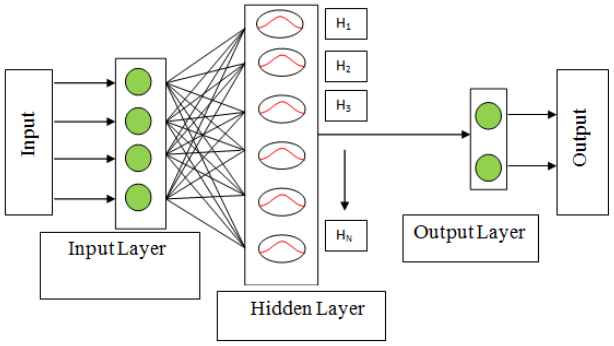

Fig 8: Structure of RBF Network

6 . RESULT AND DISCUSSION

A cantilever beam specimen with transverse crack is used to obtain the natural frequencies in ANSYS. Further the natural frequencies have been used as the training data for the neural network in MATLAB. The results obtained from both the techniques have been discussed and analyzed in this chapter. At the end of this chapter a comparative result has been shown and the errors have been found out.

A cantilever beam of dimension 800x50x8 mm was created in ANSYS. Natural Frequencies of such beam was calculated at three different mode shapes. A total of 432 sets of readings were taken. These setup was arranged according to different sets of input and output for easy use of tool in MATLAB. An Artificial Neural network was created in MATLAB. Among 432 readings, 258 readings were used for training and rest for inspection. Different performance plots were found out and error curves were plotted and comparison were shown with reference to these sets of readings obtained from neural network such as Feed Forward Back Propagation (FFBP) and Radial Basis Feed Forward Back Propagation Network (RBF).

Different modes of vibration of Beam:

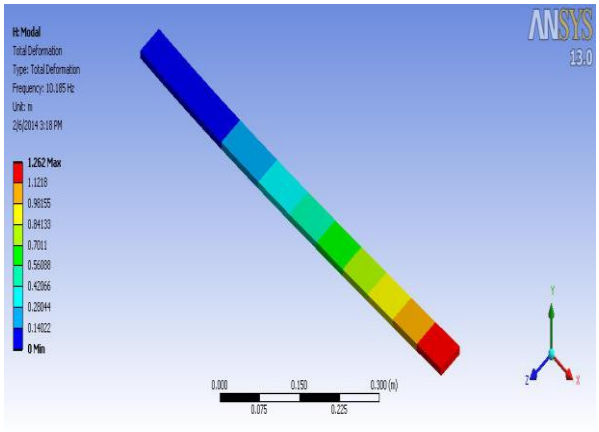

Fig. 9: Mode Shape 1 vibration

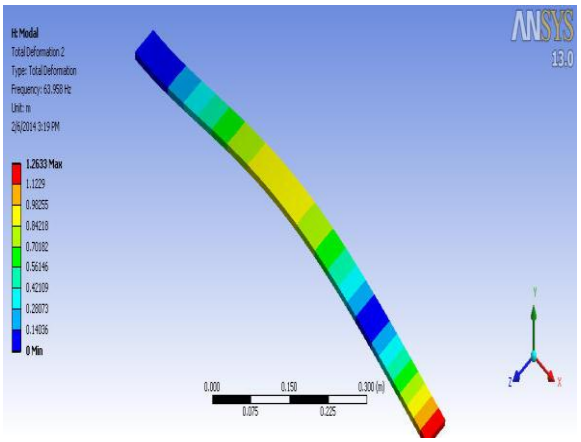

Fig. 10: Mode Shape 2 vibration

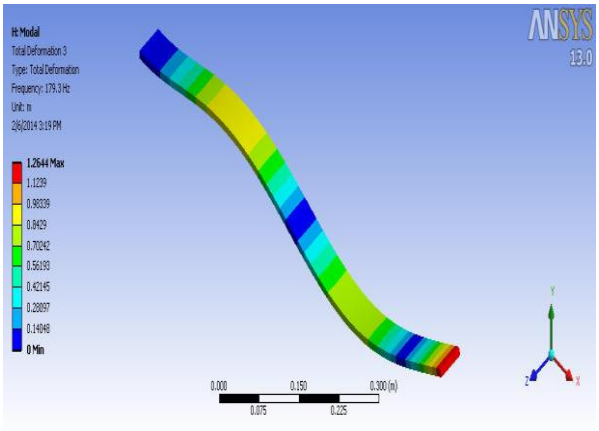

Fig. 11: Mode Shape 3 vibration

International Journal of Engineering Research & Technology (IJERT)
ISSN: 2278-0181
Vol. 6 Issue 05, May - 2017

Table 1: Observation of frequencies of vibrating beam in mode shape 1 for different location and depth of crack

							Depth						
		0.25	0.5	0.75	1	1.25	1.5	1.75	2	2.25	2.5	2.75	3
	50	10.241	10.26	10.229	10.258	10.239	10.226	10.221	10.185	10.182	10.158	10.18	10.11
	70	10.27	10.25	10.24	10.236	10.259	10.25	10.196	10.195	10.177	10.242	10.127	10.18
	90	10.256	10.245	10.242	10.242	10.233	10.23	10.249	10.194	10.196	10.193	10.112	10.082
	110	10.279	10.249	10.25	10.243	10.235	10.221	10.204	10.19	10.194	10.184	10.153	10.129
	130	10.283	10.264	10.248	10.242	10.244	10.236	10.23	10.194	10.188	10.188	10.159	10.136
	150	10.28	10.25	10.251	10.245	10.242	10.238	10.226	10.207	10.195	10.176	10.143	10.176
	170	10.271	10.251	10.247	10.251	10.247	10.24	10.23	10.232	10.233	10.189	10.233	10.154
	190	10.273	10.25	10.746	10.253	10.258	10.258	10.235	10.213	10.213	10.239	10.218	10.119
Loc	210	10.253	10.252	10.26	10.249	10.26	10.238	10.238	10.238	10.215	10.189	10.189	10.168
	230	10.263	10.25	10.265	10.255	10.256	10.253	10.232	10.223	10.219	10.176	10.176	10.176
	250	10.266	10.252	10.251	10.252	10.25	10.252	10.241	10.23	10.208	10.208	10.183	10.21
	270	10.253	10.252	10.261	10.247	10.247	10.249	10.246	10.231	10.228	10.221	10.224	10.191
	290	10.253	10.264	10.247	10.248	10.25	10.243	10.24	10.23	10.223	10.213	10.227	10.219
	310	10.255	10.251	10.257	10.249	10.246	10.242	10.243	10.232	10.227	10.223	10.217	10.21
	330	10.254	10.251	10.248	10.249	10.245	10.241	10.238	10.234	10.232	10.222	10.223	10.217
	350	10.253	10.252	10.254	10.274	10.253	10.252	10.24	10.24	10.233	10.262	10.215	10.216
	370	10.274	10.251	10.25	10.251	10.255	10.253	10.24	10.239	10.235	10.231	10.225	10.216
	390	10.253	10.252	10.253	10.249	10.249	10.25	10.244	10.24	10.234	10.231	10.232	10.226

Table 2: Observation of frequencies of vibrating beam in mode shape 2 for different location and depth of crack

							Depth						
		0.25	0.5	0.75	1	1.25	1.5	1.75	2	2.25	2.5	2.75	3
	50	64.144	64.17	64.083	64.215	64.165	64.087	64.095	63.958	63.947	63.855	64.134	63.655
	70	64.262	64.197	64.168	64.111	64.254	64.227	63.991	64.002	63.956	64.308	63.796	64.022
	90	64.189	64.164	64.165	64.161	64.138	64.208	64.21	64.073	64.015	64.118	64.057	64.903
	110	64.249	64.205	64.223	64.323	64.312	64.187	64.164	64.147	64.152	64.118	64.07	64.047
	130	64.223	64.191	64.208	64.224	64.178	64.352	64.351	64.176	64.173	64.17	64.153	64.139
	150	64.224	64.212	64.207	64.224	64.33	64.202	64.2	64.197	64.197	6.419	64.185	64.193

International Journal of Engineering Research & Technology (IJERT)
ISSN: 2278-0181
Vol. 6 Issue 05, May - 2017

	170	64.196	64.195	64.195	64.196	64.249	64.249	64.248	64.25	64.417	64.248	64.417	64.217
Loc	190	64.216	64.216	64.704	64.283	64.317	64.218	64.213	64.201	64.2	64.413	64.221	64.219
	210	64.2	64.199	64.193	64.192	64.214	64.187	64.187	64.187	64.177	64.165	64.165	64.155
	230	64.224	64.215	64.346	64.343	64.257	64.247	64.202	64.305	64.299	64.249	64.249	64.249
	250	64.245	64.204	64.2	64.199	64.212	64.213	64.193	64.154	64.101	64.101	64.108	64.105
	270	64.22	64.212	64.271	64.197	64.208	64.213	64.206	64.13	64.119	64.092	64.381	63.978
	290	64.223	64.268	64.188	64.189	64.316	64.181	64.162	64.114	64.044	63.986	64.107	64.046
	310	64.232	64.21	64.288	64.194	64.178	64.145	64.147	64.056	64.012	63.973	63.925	63.869
	330	64.254	64.205	64.184	64.236	64.186	64.102	64.073	64.025	64.001	63.879	63.915	63.852
	350	64.236	64.21	64.263	64.245	64.217	64.197	64.046	64.045	63.942	64.458	63.666	63.666
	370	64.48	64.216	64.209	64.246	64.305	64.266	64.054	64.019	63.916	63.837	63.715	63.596
	390	64.242	64.224	64.239	64.16	64.167	64.173	64.028	63.938	63.807	63.726	63.738	63.584

Table 3: Observation of frequencies of vibrating beam in mode shape 3 for different location and depth of crack

							Depth						
		0.25	0.5	0.75	1	1.25	1.5	1.75	2	2.25	2.5	2.75	3
	50	179.52	179.42	179.31	179.68	179.63	179.38	179.52	179.3	179.28	179.14	180.79	178.8
	70	179.75	179.67	179.62	179.42	179.84	179.82	179.3	179.37	179.32	180.17	179.11	179.52
	90	179.59	179.57	179.57	179.57	179.54	179.68	179.69	179.55	179.5	179.89	179.91	179.83
	110	179.72	179.72	179.71	179.85	179.85	179.71	179.71	179.71	179.72	179.73	179.76	179.73
	130	179.63	179.67	179.62	179.7	179.59	180.03	180.03	179.57	179.57	179.57	179.54	179.52
	150	179.79	179.74	179.66	179.69	179.82	179.63	179.6	179.52	179.46	179.44	179.31	179.41
Loc	170	179.76	179.66	179.67	179.68	180.03	179.99	179.95	179.9	180.76	179.66	180.76	178.97
	190	179.93	179.93	179.73	179.72	179.87	179.88	179.58	179.25	179.25	180.73	179.51	179.19
	210	179.69	179.67	179.67	179.62	179.86	179.45	179.45	179.45	179.05	178.71	178.71	178.37
	230	179.93	179.71	179.92	179.79	179.83	179.74	179.3	179.18	179.09	178.28	178.28	178.28
	250	180.02	179.69	179.67	179.7	179.65	179.3	179.47	179.23	178.72	178.72	178.58	178.78
	270	179.75	179.73	179.93	179.62	179.61	179.65	179.58	179.22	179.15	179.98	180.47	178.29
	290	179.73	179.94	179.6	179.61	179.48	179.42	179.34	179.11	179.04	178.81	179.09	178.97
	310	179.8	179.73	179.8	179.66	179.58	179.49	179.54	179.31	179.2	179.13	179	178.86

International Journal of Engineering Research & Technology (IJERT)
ISSN: 2278-0181
Vol. 6 Issue 05, May - 2017

	330	179.7	179.66	179.64	180.03	179.96	179.52	179.46	179.4	179.38	179.17	179.22	179.17
	350	179.74	179.72	179.71	179.85	179.76	179.75	179.58	179.58	179.51	182.1	179.35	179.25
	370	181.12	179.69	179.74	180.08	180.14	180.13	180.03	180.03	179.63	179.61	179.58	179.93
	390	179.71	179.72	179.72	179.7	179.7	179.64	179.7	179.69	179.68	179.68	179.69	179.7

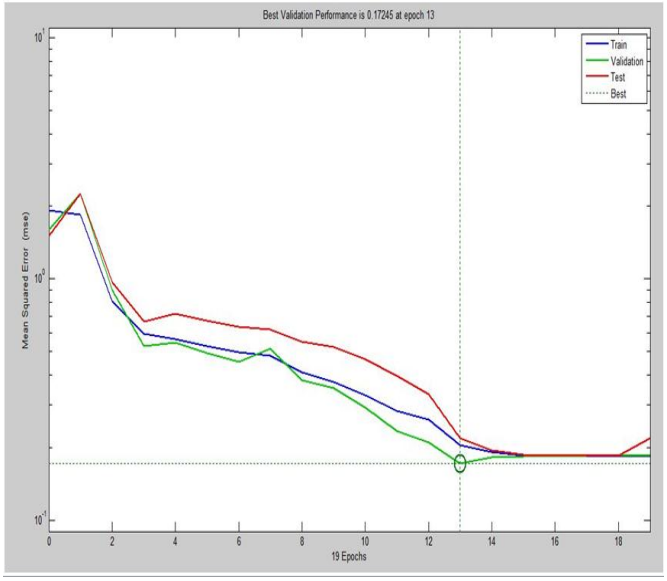

Fig 12: Performance plot of Feed Forward Back Propagation

The Levenberg-Marquardt (trainlm) training process was followed to train the neural network. The division of training data was done using the random (Dividerand) method. Since the number of values employed for testing was large in number, hence, few values were taken to depict the efficiency of the ANN model.

A regression plot is also generated which is shown in Figure for the individual results obtained between the trained, tested, and validated points against a threshold value. On plotting the values obtained from ANSYS and ANN and comparing both, it was observed that minimum difference was obtained between both of the values thus validating our training process. It was observed that after running the CFBP network for a particular number of iterations a certain value of error between the ANSYS generated values and the network generated values was obtained.

At epoch 13, the validation value matches with the best value.

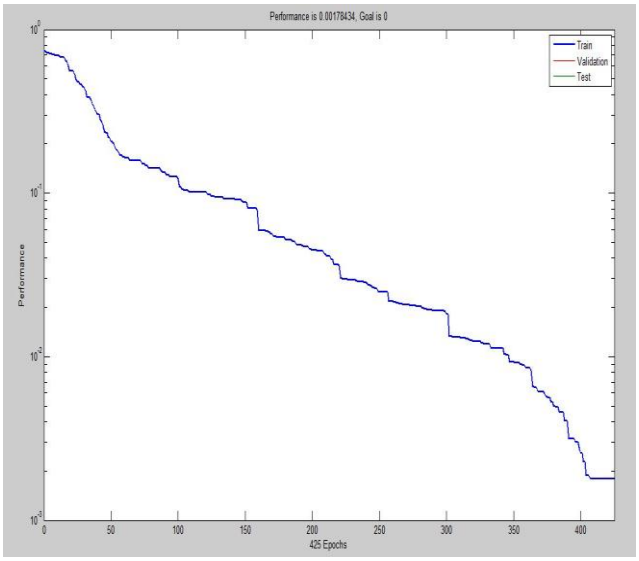

Fig 13:Performance plot of RBF Forward Back Propagation

The Radial Basis Feed Forward Back Propagation network generated a performance plot on the grounds that in an Radial Basis Feed Forward Back Propagation network a particular goal is set to be reached but the number of iterations is not fixed. For this particular case it was observed that the errors generated in all cases are of the order of 10^{-3} and the RBF network certainly yields a better result at more frequent intervals than the CFBP and the FFBP network

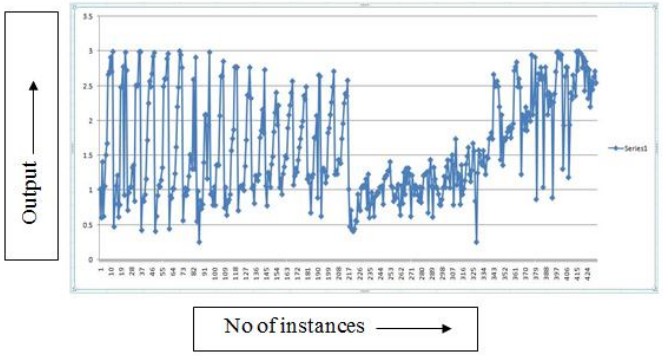

Fig 14: Output graph of RBF Forward Back Propagation

This graph is plotted between the values of output for different sets of readings, shows the output values which was found in mat lab is Feed Forward Back Propagation for corresponding readings.

International Journal of Engineering Research & Technology (IJERT)
ISSN: 2278-0181
Vol. 6 Issue 05, May - 2017

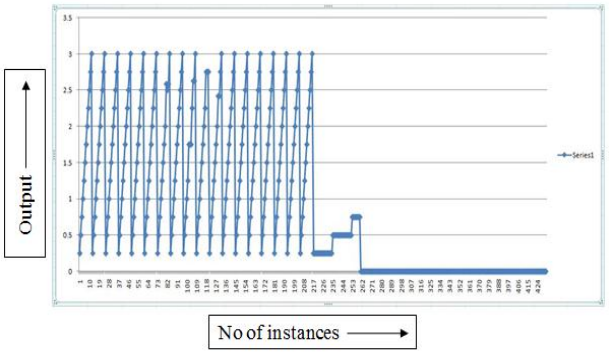

Fig 15: Output graph of RBF Forward Back Propagation

This graph is plotted between the values of output for different sets of readings, shows the output values which was found in mat lab in Radial Basis Feed Forward Back Propagation for corresponding set of readings.

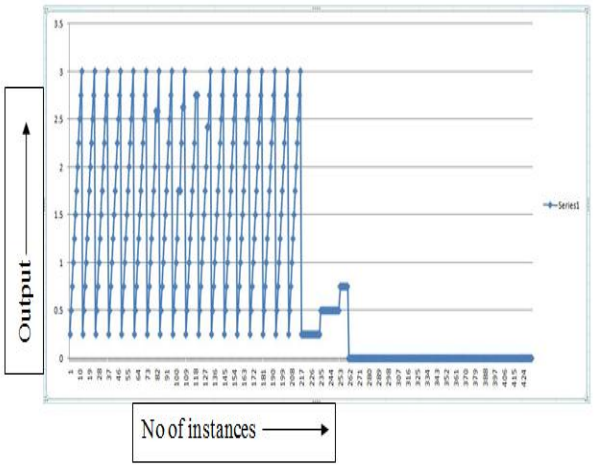

Fig16: Output graph RBF Forward Back Propagation (fewer neurons)

This graph is plotted between the values of output for different sets of readings, shows the output values which was found in mat lab in Radial Basis Feed Forward Back Propagation (fewer neurons) for corresponding set of readings.

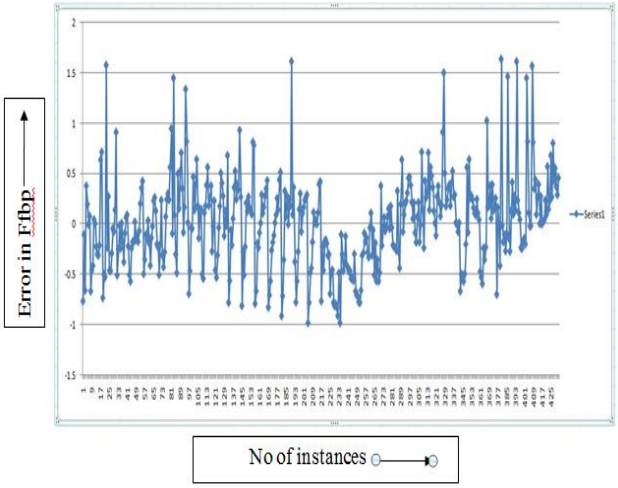

Fig 17: Error graph of Feed Forward Back Propagation

Here graph was plotted between the error in Feed Forward Back Propagation and number of instances. It was found to be maximum. Here this graph shows the value of error for different set of readings.

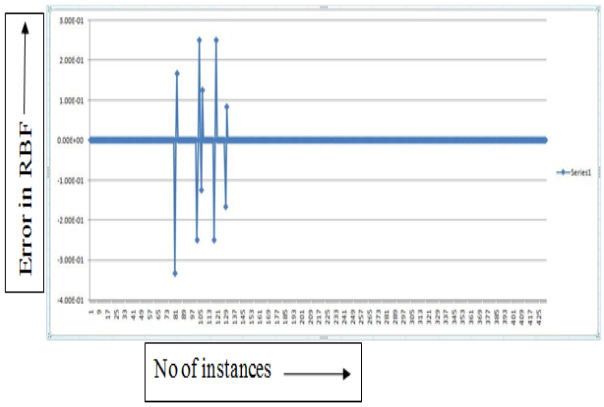

Fig 18: Error graph of Radial Basis Feed Forward Back Propagation

Here graph was plotted between the error in Radial Basis Feed Forward Back Propagation and number of instances. The error was found out to be constant for maximum sets of readings. Here this graph shows the value of error for different set of readings.

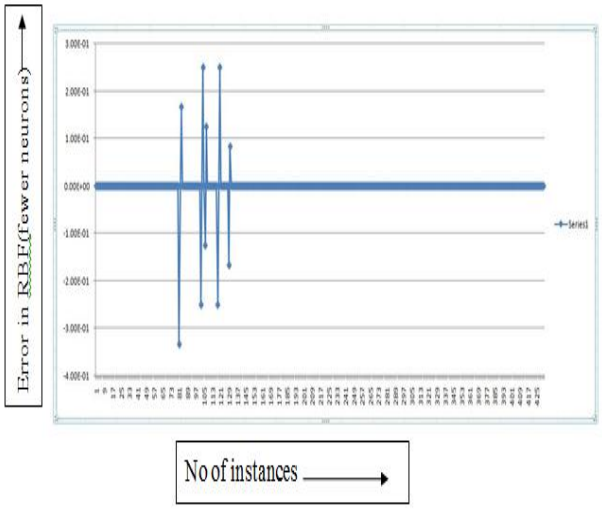

Fig 19: error graph of Radial Basis Feed Forward Back Propagation (fewer neurons)

Here graph was plotted between the error in Radial Basis Feed Forward Back Propagation (fewer neurons) and number of instances, here error is found out to be constant for maximum sets of readings. Here this graph shows the value of error for different set of readings.

International Journal of Engineering Research & Technology (IJERT)
ISSN: 2278-0181
Vol. 6 Issue 05, May - 2017

Table 4: Comparison Table between FFBP, RBF and RBF (fewer neurons)

LOCATION	OUTPUT	NETWORK ERROR			NETWORK OUTPUT		
		FFBP	RBF(EXACT FIT)	RBF(FEWER NEURONS)	FFBP	RBF(EXACT FIT)	RBF(FEWER NEURONS)
50	0.25	-0.7598	1.84E-07	7.31E-07	1.009839	0.2499	0.2499
70	0.5	-0.2972	3.82E-09	3.51E-08	0.797201	0.4999	0.499
90	0.75	-0.457	5.97E-08	6.99E-07	0.707003	0.74999	0.7499
110	1.0	-0.3739	8.87E-07	9.54E-07	0.873951	0.9999	0.999
130	1.25	-0.1702	-6.70E-08	4.32E-08	0.920255	1.249999	1.2499
150	1.5	-0.0207	-5.58E-08	1.61E-07	1.020762	1.4999	1.4999
170	1.75	0.245843	-1.50E-07	2.02E-07	1.004157	1.7499	1.7499
190	2.0	0.707923	5.79E-07	-1.95E-07	0.792077	1.9999	1.999
210	2.25	0.391951	2.29E-08	2.46E-07	1.358049	2.24999	2.2499

7. CONCLUSION

The effects of transverse cracks on the vibrating uniform cracked cantilever beam have been presented in this paper. The main purpose of this research work has been to develop a proficient technique for diagnosis of crack in a vibrating structure in short span of time. The vibration analysis has been done using theoretical and also it has been carried out through using finite element method as per ANSYS. In this analysis natural frequency plays an important role in the identification of crack. Crack has been identified in terms of crack depth and crack location. The results obtained from ANSYS are used to develop artificial intelligence techniques using three neural networks (FFBP, RBF, and CFBP). The CFBP network shows a better result than the FFBP network; the CFBP network gives the best validation performance of 0.00178434, whereas the FFBP network gives 0.17245.

It is observed that for some cases RBF network result out performs the results of the other two networks. But in general CFBP was found to be more efficient in terms of error and computational complexity. As it was observed that the predicted results of neural network technique are reasonably adequate and in agreement with the theoretical result, the developed models can be efficiently used for crack detection problems.

REFERENCES

[1] Thatoi D. N., Das H.C., Parhi D. R., "Review of Techniques for Fault Diagnosis in Damaged Structure and Engineering System", vol 2012, article id 327569.

[2] Maosen Cao, Li Cheng, Zhongqing Su, HaoXu, "A multi-scale pseudo-force model in wavelet domain for identification of damage in structural components" Mechanical Systems and Signal Processing 28 (2012) 638–659.

[3] Prashant M. Pawar, Ranjan Ganguli, "Matrix Crack Detection in Thin-walled Composite Beam using Genetic Fuzzy System" Journal of Intelligent Material Systems and Structures, Vol. 16, Issue 5, (2005) Pages: 395-409.

[4] Taghi M. and Baghmisheh V., "Crack detection in beam-like structures using genetic algorithms", Applied Soft Computing ,Vol. 8, Issue 2, (2008), Pages: 1150-1160.

[5] Maity D. and Saha A., "Damage assessment in structure from changes in static parameter using neural networks", Publisher Springer India, Issue 3, Vol. 29, (2004).

[6] Fang X., Luo H. and Tang J., "Structural damage detection using neural network with learning rate improvement", Computers & Structures, Vol. 83, Issues 25-26, (2005), Pages: 2150-2161.

[7] Sanz J., Perera R. , and Huerta C., "Fault diagnosis of rotating machinery based on auto-associative neural networks and wavelet transforms," Journal of Sound and Vibration, vol. 302, no. 4-5, pp. 981–999, 2007.

[8] Ratcliffe C.P., "Frequency and curvature based experimental method for locating damage in structures", Journal of Vibration Acoustic, 122, (2000), Pages: 324 329.

[9] Shen M.H.H. and Taylor J.E., "An identification problem for vibrating cracked beams", Journal of Sound and Vibration, Vol. 150, Issue 3, (1991), Pages: 457-484.

[10] Sahoo A.K., Zhang Y., and Zuo M.J., "Estimating crack size and location in a steel plate using ultrasonic signals and CFBP neural networks," in Proceedings of the IEEE Canadian Conference on Electrical and Computer Engineering (CCECE '08), pp. 1751–1754, May 2008.

[11] Gopikrishnan M. and Santhanam T., "Effect of different neural networks on the accuracy in iris patterns recognition," International Journal of Reviews in Computing, vol. 7, pp. 22–28, 2011.

[12] Badde D.S., Gupta A.K. and Patki V.K., "Cascade and feed forward back propagation artificial neural network models for prediction of compressive strength of ready mix concrete," IOSR Journal of Mechanical and Civil Engineering, vol. 3, pp. 1–6, 2013.